

Electron Transfer in Self-Assembled Inorganic Polyelectrolyte/Metal Nanoparticle Heterostructures

Daniel L. Feldheim, Katherine C. Grabar, Michael J. Natan,* and Thomas E. Mallouk*

Department of Chemistry, Pennsylvania State University University Park, Pennsylvania 16802

Received April 10, 1996

The way in which molecular building blocks are arranged within supramolecular structures has a marked effect on their chemical and physical properties.¹ The development of techniques for controlling the spatial arrangement of the individual components of a composite material on the nanometer and sub-nanometer levels is, therefore, crucial to the design and fabrication of advanced electronic, optical, and mechanical materials. Basic design strategies for building supramolecular systems that have appeared in recent years involve control of hydrogen bonding,² polymerization in layered solids,³ and thin-film assembly on solid supports via sequential complexation reactions⁴ or ion exchange.⁵

We recently reported a simple method for assembling multilayer thin films from single anionic sheets of lamellar inorganic solids (e.g., α -Zr(HPO₄)₂·H₂O (α -ZrP)) and organic polyelectrolyte cations (poly(allylamine hydrochloride) (PAH)).^{5c} The method is similar to one reported earlier by Decher and co-workers,^{5d} except that the replacement of organic polyanions by two-dimensional sheets prevents mixing of the components of adjacent layers.^{5g} We describe here an extension of this layer-by-layer assembly scheme to the fabrication of metal–insulator–gold nanocluster–insulator–metal (MINIM) heterostructures. The MINIM structure is analogous to two parallel plate capacitors in series. An important difference between a MINIM device and a conventional, macroscale capacitor is that the small gold particle diameter (2.5 ± 1.5 nm) produces capacitances of only $\sim 10^{-18}$ F, thus allowing the observation of single electron charging effects at ambient temperatures. Previous work describing these effects is summarized briefly below.⁶

* To whom correspondence should be addressed.

(1) (a) Ozin, G. A. *Adv. Mater.* **1992**, *4*, 612. (b) Mann, S. *J. Mater. Chem.* **1995**, *5*, 935. (c) Lakes, R. *Nature* **1993**, *361*, 511. (d) Spaepen, F. *Science* **1987**, *23*, 1010. (e) Bard, A. J. *Integrated Chemical Systems*; John Wiley & Sons: New York, 1994. (f) Whitesides, G. M.; Mathias, J. P.; Seto, C. T. *Science* **1991**, *254*, 1312.

(2) (a) Panunto, T. W.; Urbanczyk-Lipkowska, Z.; Johnson, R.; Etter, M. C. *J. Am. Chem. Soc.* **1987**, *109*, 7786. (b) Marsh, A.; Nolen, E. G.; Gardinier, K. M.; Lehn, J.-M. *Tetrahedron Lett.* **1994**, *35*, 279. (c) Gallant, M.; Viet, M. T. P.; Wuest, J. D. *J. Org. Chem.* **1991**, *56*, 2284. (d) Whitesell, J. K.; Davis, R. E.; Wong, M.-S.; Chang, N.-L. *J. Am. Chem. Soc.* **1994**, *116*, 523. (e) Simard, M.; Su, D.; *J. Am. Chem. Soc.* **1991**, *113*, 4696. (f) Seto, C. T.; Whitesides, G. M. *J. Am. Chem. Soc.* **1990**, *112*, 2440. (g) Mathias, J. P.; Seto, C. T.; Simanek, E. E.; Whitesides, G. M. *J. Am. Chem. Soc.* **1994**, *116*, 1725.

(3) (a) Mehrotra, V.; Giannelis, E. P. *Solid State Comm.* **1991**, *77*, 155. (b) Feldheim, D. L.; Mallouk, T. E. Submitted for publication. (c) Cao, G.; Mallouk, T. E. *J. Solid State Chem.* **1991**, *94*, 59. (d) Thompson, M. E. *Chem. Mater.* **1994**, *6*, 1168. (e) Kanatzidas, M. G.; Wu, C.-G.; Marcy, H. O. *Chem. Mater.* **1990**, *2* (3), 222. (f) Kanatzidas, M. G.; Bissessur, R.; DeGroot, D. C. *Chem. Mater.* **1993**, *5* (3), 595.

(4) (a) Snover, J. L.; Thompson, M. E. *J. Am. Chem. Soc.* **1994**, *116*, 756. (b) Lee, H.; Kepley, L. J.; Hong, H.-G.; Mallouk, T. E. *J. Am. Chem. Soc.* **1988**, *110*, 618. (c) Cao, G.; Hong, H.-G.; Mallouk, T. E. *Acc. Chem. Res.* **1992**, *25*, 420. (d) Putvinski, T. M.; Schilling, M. L.; Katz, H. E.; Chidsey, C. E. D.; Mujisce, A. M.; Emerson, A. B. *Langmuir* **1990**, *6*, 1567. (e) Katz, H. E.; Schilling, M. L.; Chidsey, C. E. D.; Putvinski, T. M.; Hutton, R. S. *Chem. Mater.* **1991**, *3*, 699.

(5) (a) Schmitt, J.; Decher, G.; Dressick, W. J.; Brandow, S. L.; Geer, R. E.; Shashidhar, R.; Calvert, J. M. Submitted for publication. (b) Kleinfeld, E. R.; Ferguson, G. S. *Science* **1994**, *265*, 370. (c) Ferreira, M.; Rubner, M. F. *Macromolecules* **1995**, *28*, 7107. (d) Decher, G.; Hong, J. D.; Schmitt, J. *Thin Solid Films* **1992**, *210/211*, 831. (e) Keller, S. W.; Kim, H. N.; Mallouk, T. E. *J. Am. Chem. Soc.* **1994**, *116*, 8817. (f) Hong, J. D.; Lowack, K.; Schmitt, J.; Decher, G. *Prog. Colloid Polym. Sci.* **1993**, *93*, 98. (g) Kaschak, D. M.; Mallouk, T. E. *J. Am. Chem. Soc.* **1996**, *118*, 4222.

Classically, the capacitance of a metal–insulator–spherical metal particle junction is given by (1),⁶ⁱ where ϵ_0 is the vacuum

$$C = 4\pi\epsilon_0\epsilon_r(1 + r/2L) \quad (1)$$

permittivity constant, ϵ is the dielectric constant of the insulator, r is the particle radius, and L is the junction thickness. The work done in charging the junction is related to the capacitance by (2), where Q is the charge on the capacitor. In the small-

$$W = Q^2/2C \quad (2)$$

particle limit (< 10 nm) the voltage (W/Q) needed to charge the capacitor by a single electron becomes experimentally observable—on the order of tens to hundreds of millivolts. (Thus, Q in eq (2) becomes e , the charge of a single electron.) This leads to a high impedance region (the “Coulomb gap”) in the i - V curve of the junction. However, one further requirement is that kT must be less than $e^2/2C$ in order to avoid thermal tunneling of electrons across the gap. To date, single electron charging has been observed mainly at low temperatures (< 77 K), in devices fabricated using electron beam lithography,^{6c} or by placing the tip of a scanning tunneling microscope over a sputtered metal island film^{6b} or colloidal particle.^{6a,j,m} Below we describe the fabrication of large arrays of single electron tunneling devices by simple wet chemical methods.

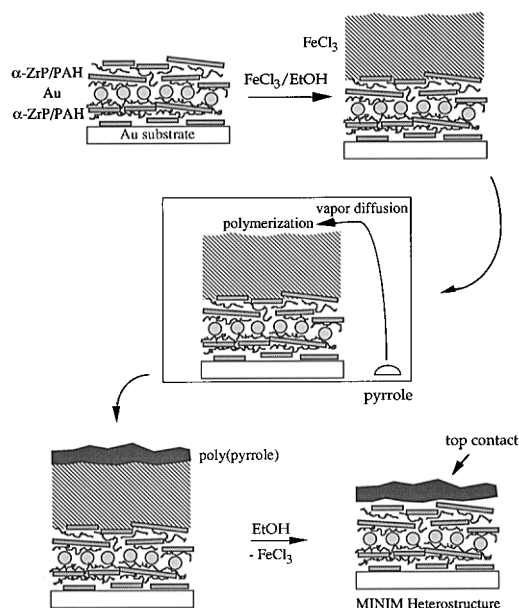
MINIM devices were made by first priming the surface of a gold substrate with 2-mercaptoethylamine.^{5a} Insulating layers of α -ZrP and PAH were adsorbed (terminating in cationic PAH) until the desired thickness, typically 30–100 Å as measured by ellipsometry, was obtained. The substrate was then placed in an aqueous solution of 2.5 ± 1.5 nm citrate-stabilized gold particles for 12 h.⁷ The anionic particles have a high affinity for amine functionalities such as those contained in PAH.⁷ The remaining half of the double junction was constructed by simply reversing the adsorption sequence just described (i.e., PAH, α -ZrP, etc.).

Ellipsometric measurements (see the supporting information) show the expected film thicknesses for (α -ZrP/PAH) multilayers.^{5c,g} An interesting feature of these data is the apparent increase in film thickness of 60–80 Å following the adsorption of 2.5 nm gold particles. The increase, which is calculated using a film refractive index (1.54) appropriate for organic materials, is 2–3 times the particle diameter as determined by transmission electron microscopy.⁷ It reflects the markedly different optical constants of the gold nanoparticles, as well as their actual thickness and surface coverage. Irrespective of the detailed

(6) (a) Dorogi, M.; Gomez, J.; Osifchin, R.; Andres, R. P.; Reifenberger, R. *Phys. Rev. B* **1995**, *52*, 9071. (b) Amman, M.; Field, S. B.; Jaklevic, R. C. *Phys. Rev. B* **1993**, *48*, 12104. (c) Fulton, T. A.; Dolan, G. J. *Phys. Rev. Lett.* **1987**, *59*, 109. (d) Amman, M.; Wilkins, R.; Ben-Jacob, E.; Maker, P. D.; Jaklevic, R. C. *Phys. Rev. B* **1991**, *43*, 1146. (e) Krans, J. M.; van Ruitenbeek, J. M.; Fisun, V. V.; Yanson, I. K.; de Jongh, L. J. *Nature* **1995**, *375*, 767. (f) Averin, D. V.; Likharev, K. K. *J. Low Temp. Phys.* **1986**, *62*, 345. (g) Ashoori, R. C.; Stormer, H. L.; Weiner, J. S.; Pfeiffer, L. N.; Pearton, S. J.; Baldwin, K. W.; West, K. W. *Phys. Rev. Lett.* **1992**, *68*, 3088. (h) Mullen, K.; Ben-Jacob, E.; Jaklevic, R. C.; Schuss, Z. *Phys. Rev. B* **1988**, *37*, 98. (i) Barner, J. B.; Ruggerio, S. T. *Phys. Rev. Lett.* **1987**, *59*, 807. (j) Osifchin, R. G.; Mahoney, W.; Andres, R. P.; Dorogi, M.; Reifenberger, R. G.; Feng, S.; Henderson, J. I.; Bein, T.; Kubiak, C. P. *Polym. Mater. Sci. Eng.* **1995**, *73*, 208. (k) *Single Charge Tunneling*; Grabert, H.; Devoret, M. H., Eds.; NATO ASI Series B; Plenum Press: New York, 1991; Vol. 294. (l) Raven, M. S. *Phys. Rev. B* **1984**, *29*, 6218. (m) Andres, R. P.; Bein, T.; Dorogi, M.; Feng, S.; Henderson, J. I.; Kubiak, C. P.; Mahoney, W.; Osifchin, R. G.; Reifenberger, R. *Science* **1996**, *272*, 1323.

(7) (a) Grabar, K. C.; Smith, P. C.; Musick, M. D.; Davis, J. A.; Walter, D. G.; Jackson, M. A.; Guthrie, A. P.; Natan, M. J. *J. Am. Chem. Soc.* **1996**, *118*, 1148. (b) Grabar, K. C.; Allison, K. J.; Baker, B. E.; Bright, R. M.; Brown, K. R.; Freeman, R. G.; Fox, A. P.; Keating, C. D.; Musick, M. D.; Natan, M. J. *Langmuir*, in press. (c) The gold cluster coverage was estimated to be ca. 1.5×10^{11} cm⁻² from UV–vis spectroscopy on (α -ZrP/PAH)₂-coated glass substrates.

Scheme 1. Illustration of the Polymerization of Pyrrole To Form a Top Contact in Metal–Insulator–Nanocluster–Insulator–Metal (MINIM) Devices



nature of the thickness change, ellipsometry clearly provides a qualitative measure of gold particle adsorption. Successive layers of PAH and α -ZrP can be grown on top of the 2.5 nm gold particles, and thickness changes are similar to those of the layers adsorbed prior to particle deposition. More quantitative evidence for spatially-defined (α -ZrP/PAH)/Au nanocluster/(PAH/ α -ZrP) layers was obtained from X-ray photoelectron spectra (XPS). Spectra acquired on silicon substrates with [(α -ZrP/PAH)₁/12 nm Au cluster/(PAH/ α -ZrP)₂] multilayers show an attenuated gold 4f signal compared to [(α -ZrP/PAH)₁/Au nanocluster] films. In addition, relative Au/Zr, Au/Si and Zr/Si, intensities calculated from a layered film model agree quantitatively with the observed values (see the supporting information). These data support a film structure in which the gold clusters lie on top of a PAH layer and then are completely covered by subsequent layers of PAH and α -ZrP, resulting in the sandwich structure shown in Scheme 1.

In order to measure the current–voltage (*i*–*V*) behavior of the device, ohmic contacts were made as shown in Scheme 1 and in the inset to Figure 1.⁸ For a junction thickness of 80 Å and a particle radius of 1.25 nm, the capacitance of a double tunnel junction device calculated from (1) is 4.5×10^{-19} F. A Coulomb gap, $e/C = 360$ mV, should be observable at room temperature because it is many times greater than kT . A typical *i*–*V* curve for such a MINIM structure is presented in Figure 1A.⁹ The high impedance region is evident on both sides of 0 V, and represents the average charging potential ($\pm e/2C$) of each particle of the double junction array by a single electron. Once enough energy is supplied to charge the particles, electrons tunnel more readily through the junction, resulting in the square-law dependence of the current rise ($R = 0.99$) on either side of the gap.^{6h} These data were obtained at room temperature and were reproducible as the potential was scanned from -1 to $+1$

(8) One contact was made by attaching a copper wire to a bare region of the gold substrate with silver epoxy. A reliable top contact has proven difficult without shorting with the underlying substrate. Our most successful approach to date has been to use an organic conducting polymer as the contact. This was accomplished by depositing a thin layer of FeCl_3 (0.1 M in 95% $\text{CH}_3\text{CH}_2\text{OH}$) onto the substrate from solution, allowing the solvent to evaporate, and exposing the substrate to pyrrole vapor (Scheme 1). The Fe^{III} initiates the polymerization of a layer of electronically conducting polypyrrole. The FeCl_3 layer was then removed by placing the substrate in a solution of 95% $\text{CH}_3\text{CH}_2\text{OH}$.

(9) *i*–*V* curves were acquired with a Princeton Applied Research Model 173 potentiostat and MacLab electrochemical software version 1.3.

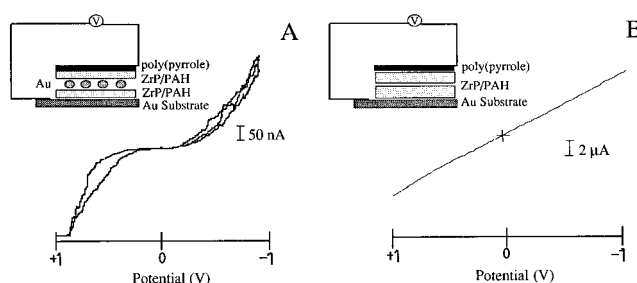


Figure 1. (A) Current–voltage curves for a [(α -ZrP/PAH)₂/2.5 nm Au clusters/(PAH/ α -ZrP)₂]/poly(pyrrole) MINIM device (see inset), scan rate 100 mV/s. (B) Current–voltage curve for the same device as in (A) without the 2.5 nm Au adsorption step (i.e., [(α -ZrP/PAH)₄]/poly(pyrrole), scan rate 100 mV/s.

V. Figure 1B shows the *i*–*V* behavior of a device of similar thickness in the absence of the gold particles. The linear curve is typical of ohmic devices.¹⁰

The versatility of the sequential assembly procedure described above provides a convenient means of tuning the Coulomb gap potential. Changing the insulator thickness from 80 to 30 Å, by using fewer inorganic/polyelectrolyte layer pairs, decreases the gap width from 400 to 275 mV. These values agree reasonably well with those calculated from (1) and (2) (360 and 320 mV, respectively).¹¹ In addition, the electronic properties of these devices might potentially be altered by assembling two dissimilar dielectric materials around the gold colloids or by assembling multilayers of gold clusters.^{5a,12} Such devices are predicted to display single electron transfer current steps in the *i*–*V* curve (the “Coulomb staircase”).⁶ We are currently examining the *i*–*V* characteristics of these systems.

In conclusion, thin films of insulator–colloidal gold particle–insulator heterostructures have been assembled on solid supports. The observation of a high-impedance Coulomb gap indicates that there is an insignificant density of short circuits in a 1 cm² array containing approximately 10^{11} parallel tunnel junctions. Significantly, these structures and electrical contacts were assembled exclusively by benchtop, wet chemical techniques. The ability to control the spatial organization of the individual components of the composite on the nanometer level has provided access to some of the interesting electronic properties of nanoscopic systems.

Acknowledgment. This work was supported by grants from the National Science Foundation (CHE-9529202), the Office of Naval Research (Lawrence Berkeley Laboratory Molecular Design Institute), and the Advanced Research Projects Administration. D.L.F. gratefully acknowledges the National Science Foundation postdoctoral fellowship program (Grant CHE-9504672). K.C.G. acknowledges support from an Eastman Kodak Co. fellowship. The authors also thank Vince Bojan and Professor Carlo Pantano for performing the XPS measurements.

Supporting Information Available: Plots of ellipsometric film thickness vs layer number for three representative devices, and XPS data and analysis (8 pages). See any current masthead page for ordering and Internet access instructions.

JA9612007

(10) This is an important result since polypyrrole has been shown previously to act as an ohmic, non-ohmic, or rectifying contact depending on the polymerization conditions, film thickness, conductivity, etc. See for example: Ingnas, O.; Lundstrom, I. *Synth. Met.* **1984**, *10*, 5.

(11) Calculated using a film dielectric constant of 3.0; see: Kepley, L. J.; Sackett, D. D.; Bell, C. M.; Mallouk, T. E. *Thin Solid Films* **1992**, *208*, 132.

(12) (a) Terrill, R. H.; Postlewaite, T. A.; Chen, C.-H.; Poon, C. D.; Terzis, A.; Chen, A.; Hutchison, J. E.; Clark, M. R.; Wignall, G.; Londono, J. D.; Superfine, R.; Falvo, M.; Johnson, C. S., Jr.; Samulski, E. T.; Murray, R. W. *J. Am. Chem. Soc.* **1995**, *117*, 12537. (b) Hostetler, M. J.; Green, S. J.; Stokes, J. J.; Murray, R. W. *J. Am. Chem. Soc.* **1996**, *118*, 4212.

(13) Somorjai, G. A. *Introduction To Surface Chemistry and Catalysis*; John Wiley & Sons, Inc.: New York, 1994; p 382.